Four-Component Perovskites in A–R–Fe–O Systems at 1200°C (A — Alkaline-Earth, R — Rare-Earth Metal)

O. Zaremba*, V. Hrytsan and R. Gladyshevskii

Department of Inorganic Chemistry, Ivan Franko National University of Lviv, Kyryla i Mefodiya St., 6, 79005 Lviv, Ukraine

The formation of four-component perovskites in the A–R–Fe–O systems, where A is an alkaline-earth and R a rare-earth metal, was studied on the basis of the analysis of 36 polycrystalline samples synthesized by a multi-stage solid-state reaction method and annealed at 1200°C. X-ray diffraction was chosen as the main method of investigation. The existence of $A_{0.5}R_{0.5}FeO_3$ ternary compounds with $CaTiO_3$-type perovskite structures (Pearson symbol $cP5$, space group Pm-$3m$) was shown in the {Ca,Sr}–R–Fe–O systems, i.e., $Ca_{0.5}Pr_{0.5}FeO_3$ ($a = 3.8501(3)$ Å), $Ca_{0.5}Nd_{0.5}FeO_3$ ($a = 3.8486(4)$ Å), $Sr_{0.5}Pr_{0.5}FeO_3$ ($a = 3.8783(4)$ Å), $Sr_{0.5}Nd_{0.5}FeO_3$ ($a = 3.8752(4)$ Å), $Sr_{0.5}Sm_{0.5}FeO_3$ ($a = 3.8651(4)$ Å), and $Sr_{0.5}Eu_{0.5}FeO_3$ ($a = 3.8653(2)$ Å). The remaining $Ca_{0.5}R_{0.5}FeO_3$ samples contained as main phase $R_{1-x}Ca_xFeO_3$ solid solutions with orthorhombic structure (x up to 0.25, $GdFeO_3$ type, $oP20$, $Pnma$), whereas the $Sr_{0.5}R_{0.5}FeO_3$ samples contained $Sr_xR_{1-x}FeO_3$ solid solutions with cubic structure (x up to 0.4, $CaTiO_3$ type). Annealing of Ba-containing samples at 1200°C led to the formation of $Ba_{1-x}R_xFeO_3$ ($x \simeq 0.15$) solid solutions based on the $BaFeO_3$ phase ($CaTiO_3$ type) for light rare-earth metals.

topics: alkaline-earth metal, rare-earth metal, iron, perovskite

1. Introduction

Perovskites form a huge family of compounds derived from the structure of the $CaTiO_3$ type. They possess numerous unique physical properties, among which are: colossal magnetoresistance, magnetic ordering, thermal, optical, dielectric, piezoelectric, and ferroelectric properties, electronic conductivity, superconductivity, catalytic activity, etc. Nowadays, perovskites, especially those containing alkaline-earth (A) and rare-earth (R) metals, represent an important class of fundamental materials due to their widespread application in various branches of technology [1–3]. Thus, a detailed study of the relationship between the conditions of formation, composition, crystal structures, and properties of perovskites is of great interest.

Analysis of literature data on A–R–Fe–O systems [4] showed the formation of four-component $(A,R)FeO_3$ perovskites in the vast majority of the cases. In the Ca–R–Fe–O systems, such phases exist for R = light rare-earth metal (except Pm and Eu) and Dy and belong to the $CaTiO_3$ or $GdFeO_3$ structure types. A similar situation is observed in the Sr–R–Fe–O systems, i.e., $(Sr,R)FeO_3$ phases are formed for R = light rare-earth metal (except Pm) and Dy and their structures can be described by the $CaTiO_3$, $GdFeO_3$, $LaAlO_3$, $Ba(Pb_{0.5}Bi_{0.5})O_3$,

or $Sr(Fe_{0.5}Ru_{0.5})O_3$ types. Regarding the Ba–R–Fe–O systems, there is information about the formation of $(Ba,R)FeO_3$ phases with most R elements (except Pm, Eu, Dy, and Ho), and all of them belong to the $CaTiO_3$ type. We noticed that the phases described above differ not only in their structures but also in the conditions of formation and A/R ratio, which motivated us to carry out a systematic study of the $AFeO_3$–$RFeO_3$ cross-sections.

This study follows up an investigation of ceramic samples of the A–R–Fe–O systems synthesized at 1000°C [5]. As a result of X-ray diffraction studies, the presence of four-component phases $R_{1-x}Ca_xFeO_3$ ($x \simeq 0.15$) with $GdFeO_3$-type perovskite structures ($oP20$, $Pnma$) was discovered in the Ca–R–Fe–O systems. We also showed that $Sr_{1-x}R_xFeO_3$ ($x \simeq 0.20$) phases with the $CaTiO_3$ structure type ($cP5$, Pm-$3m$) and $R_{1-x}Sr_xFeO_3$ ($x \simeq 0.10$) phases with the $GdFeO_3$ structure type are formed on the $SrFeO_3$–$RFeO_3$ cross-sections of the Sr–R–Fe–O systems. The formation of four-component perovskites in the Ba–R–Fe–O systems was not observed under the conditions of that investigation. The aim of this work was to find the existence of four-component perovskites in the A–R–Fe–O systems at a higher temperature (1200°C).

2. Experimental

Samples of nominal composition $A_{0.5}R_{0.5}FeO_3$ (A = Ca, Sr or Ba, R = Pr, Nd, Sm, Eu, Gd, Tb, Dy, Ho, Er, Tm, Yb or Lu) were obtained by a multi-stage solid-state synthesis from powders of alkaline-earth metal carbonates, rare-earth metal and iron(III) oxides of high purity. At the initial step, appropriate quantities of the reagents were mixed and heated in a muffle furnace SNOL-1.6 at 1000°C for 24 h to decompose the carbonates. Then the mixtures were ground, pressed into tablets ($m \simeq 0.5$ g), and again sintered under the same conditions. Finally, all the samples were ground, pressed, and annealed in a tube furnace SNOL-0.3/1250 at 1200°C for 8 h.

X-ray powder diffraction data, collected on a DRON-2.0M diffractometer (Fe K_α radiation, $20 \leq 2\theta \leq 80$, 1°/min), were used for phase and structural analysis performed by the Rietveld method. The refinement of the structural param-eters (unit-cell parameters; atom coordinates; site occupancies; scale factor; zero shift; FWHM parameters U, V, W; mixing parameter; asymmetry of peaks, etc.) was carried out using the DBWS program [6]. To evaluate the quality of the refinement, the reliability Bragg factor (R_B) was applied.

3. Results and discussion

As a result of the phase analysis of the polycrystalline samples with nominal composition $A_{0.5}R_{0.5}FeO_3$ annealed at 1200°C, the formation of the ternary phases $Ca_{0.5}Pr_{0.5}FeO_3$ and $Ca_{0.5}Nd_{0.5}FeO_3$, which crystallize with cubic $CaTiO_3$-type structures ($cP5$, Pm-$3m$), was discovered. The refined crystallographic parameters of these perovskites are presented in Table I. The structural model for the refinements was taken from [7]. Diffraction patterns of the corresponding single-phase samples are shown in Fig. 1. The other $Ca_{0.5}R_{0.5}FeO_3$ samples contained, as
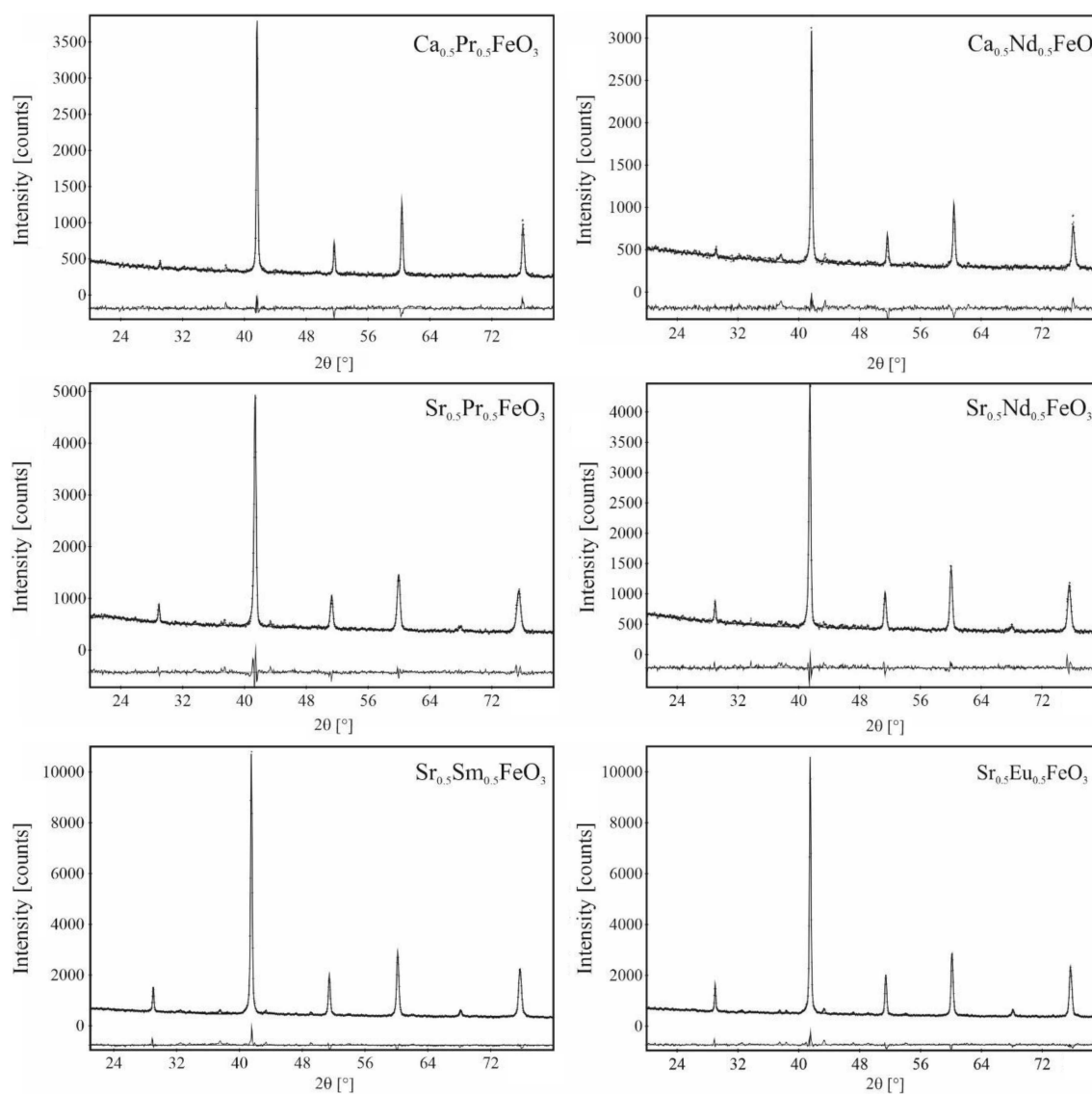
Fig. 1. XRD powder patterns of $A_{0.5}R_{0.5}FeO_3$ samples annealed at 1200°C.

TABLE I

Results of XRD phase and structural analysis of $A_{0.5}R_{0.5}FeO_3$ samples annealed at 1200°C (structure type $CaTiO_3$, Pearson symbol $cP5$, space group Pm-$3m$, content = 100 wt%).

Nominal/ refined composition	Unit-cell parameter a [Å]	R_B
$Ca_{0.5}Pr_{0.5}FeO_3/$ $Ca_{0.47(2)}Pr_{0.53(2)}FeO_3$	3.8501(3)	0.081
$Ca_{0.5}Nd_{0.5}FeO_3/$ $Ca_{0.46(2)}Nd_{0.54(2)}FeO_3$	3.8486(4)	0.097
$Sr_{0.5}Pr_{0.5}FeO_3/$ $Sr_{0.54(3)}Pr_{0.46(3)}FeO_3$	3.8783(4)	0.095
$Sr_{0.5}Nd_{0.5}FeO_3/$ $Sr_{0.51(3)}Nd_{0.49(3)}FeO_3$	3.8752(4)	0.095
$Sr_{0.5}Sm_{0.5}FeO_3/$ $Sr_{0.45(2)}Sm_{0.55(2)}FeO_3$	3.8651(4)	0.094
$Sr_{0.5}Eu_{0.5}FeO_3/$ $Sr_{0.46(1)}Eu_{0.54(1)}FeO_3$	3.8653(2)	0.047

the main phase, $R_{1-x}Ca_xFeO_3$ solid solutions based on the $RFeO_3$ phases (x up to 0.25, $GdFeO_3$ type, $oP20$, $Pnma$). The unit-cell volumes of the $R_{1-x}Ca_xFeO_3$ phases versus the atomic number of the rare-earth element (R) are displayed in Fig. 2. The cell parameters decrease linearly with the increasing atomic number of the rare-earth metal, in agreement with Vegard's law. Figure 3 shows the crystal structures of the cubic $CaTiO_3$ and orthorhombic $GdFeO_3$ perovskite types.

The results of the phase analysis of the polycrystalline samples of nominal composition $Sr_{0.5}R_{0.5}FeO_3$ annealed at 1200°C are presented in Table II. In this case, the formation of ternary $Sr_{0.5}A_{0.5}FeO_3$ phases, characterized by the cubic $CaTiO_3$ perovskite structure, was observed for A = Pr, Nd, Sm, and Eu (see Tables I and II and Fig. 1). The samples with other rare-earth elements (except Er) were two-phase. They were contained in equilibrium $Sr_xR_{1-x}FeO_3$ solid solutions (based on the $SrFeO_3$ phase with the structure of cubic perovskite, x up to 0.4) and the corresponding $RFeO_3$ phase (with the structure of orthorhombic perovskite). It was not possible to trace some tendency of the cell parameters for the $Sr_xR_{1-x}FeO_3$ solid solutions, since the replacement of larger R atoms by smaller ones (from Gd to Lu) was accompanied by an increase of x (the content of Sr atoms).

The qualitative phase analysis of the $Ba_{0.5}R_{0.5}FeO_3$ samples annealed at 1200°C revealed the formation of four-component $Ba_{1-x}R_xFeO_3$ ($x \simeq 0.15$) perovskites with $CaTiO_3$-type structures for R = light rare-earth metals only. Samples with heavy rare-earth elements (R = Tb, Tm) contained more than three phases. The $Ba_{0.5}Yb_{0.5}FeO_3$ and $Ba_{0.5}Lu_{0.5}FeO_3$ samples, in turn, contained $\approx$ 60 wt% of the $BaFe_2O_4$ phase (own structure
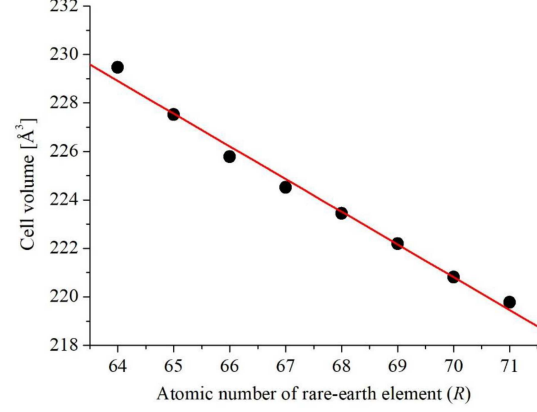
Fig. 2. Unit-cell volume of $R_{1-x}Ca_xFeO_3$ phases versus atomic number of the rare-earth element (R).
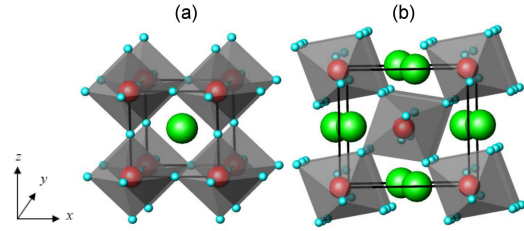
Fig. 3. Crystal structures of the cubic $CaTiO_3$ (a) and orthorhombic $GdFeO_3$ (b) perovskite types.

type) and $\approx$ 40 wt% of the corresponding R_2O_3 sesquioxide (($Mn_{0.5}Fe_{0.5})_2O_3$ type), but no traces of a perovskite phase.

A comparison of the results obtained here with those from investigating the samples annealed at 1000°C [5] indicates an increased tendency to form perovskite phases in the A–R–Fe–O systems with the increase in the temperature to 1200°C.

4. Conclusions

The polycrystalline samples of $A_{0.5}R_{0.5}FeO_3$ nominal composition were synthesized by a solid-state reaction method at 1200°C and investigated using X-ray phase and structural analysis. In the result the existence of $A_{0.5}R_{0.5}FeO_3$ compounds with $CaTiO_3$-type perovskite structures (Pearson symbol $cP5$, space group Pm-$3m$) was indicated in the Ca,Sr–R–Fe–O systems: $Ca_{0.5}Pr_{0.5}FeO_3$, $Ca_{0.5}Nd_{0.5}FeO_3$, $Sr_{0.5}Pr_{0.5}FeO_3$, $Sr_{0.5}Nd_{0.5}FeO_3$, $Sr_{0.5}Sm_{0.5}FeO_3$, and $Sr_{0.5}Eu_{0.5}FeO_3$. Other Ca-containing samples contained $R_{1-x}Ca_xFeO_3$ solid solutions with orthorhombic structure (x up to 0.25, $GdFeO_3$ type, $oP20$, $Pnma$), as a main phase. For Sr-containing samples it was $Sr_xR_{1-x}FeO_3$ solid solutions with cubic structure (x up to 0.4, $CaTiO_3$ type, $cP5$, Pm-$3m$), whereas for Ba-containing samples — $Ba_{1-x}R_xFeO_3$ solid solutions (x up to 0.15) based on the $BaFeO_3$ phase ($CaTiO_3$ type) for light rare-earth metals only.

TABLE II

Results of XRD phase analysis of $Sr_{0.5}R_{0.5}FeO_3$ samples annealed at 1200°C.

Nominal composition	XRD composition	Structure type	Pearson symbol	Space group	Content [wt%]
$Sr_{0.5}Pr_{0.5}FeO_3$	$Sr_{0.54(3)}Pr_{0.46(3)}FeO_3$	$CaTiO_3$	$cP5$	Pm-$3m$	100
$Sr_{0.5}Nd_{0.5}FeO_3$	$Sr_{0.51(3)}Nd_{0.49(3)}FeO_3$	$CaTiO_3$	$cP5$	Pm-$3m$	100
$Sr_{0.5}Sm_{0.5}FeO_3$	$Sr_{0.45(2)}Sm_{0.55(2)}FeO_3$	$CaTiO_3$	$cP5$	Pm-$3m$	100
$Sr_{0.5}Eu_{0.5}FeO_3$	$Sr_{0.46(1)}Eu_{0.54(1)}FeO_3$	$CaTiO_3$	$cP5$	Pm-$3m$	100
$Sr_{0.5}Gd_{0.5}FeO_3$	$Sr_{0.62(2)}Gd_{0.38(2)}FeO_3$	$CaTiO_3$	$cP5$	Pm-$3m$	82.0
	$GdFeO_3$	$GdFeO_3$	$oP20$	$Pnma$	18.0
$Sr_{0.5}Tb_{0.5}FeO_3$	$Sr_{0.60(3)}Tb_{0.40(3)}FeO_3$	$CaTiO_3$	$cP5$	Pm-$3m$	68.9
	$TbFeO_3$	$GdFeO_3$	$oP20$	$Pnma$	31.1
$Sr_{0.5}Dy_{0.5}FeO_3$	$Sr_{0.61(2)}Dy_{0.39(2)}FeO_3$	$CaTiO_3$	$cP5$	Pm-$3m$	67.2
	$DyFeO_3$	$GdFeO_3$	$oP20$	$Pnma$	32.8
$Sr_{0.5}Ho_{0.5}FeO_3$	$Sr_{0.68(2)}Ho_{0.32(2)}FeO_3$	$CaTiO_3$	$cP5$	Pm-$3m$	61.7
	$HoFeO_3$	$GdFeO_3$	$oP20$	$Pnma$	38.3
$Sr_{0.5}Er_{0.5}FeO_3$	$Sr_{0.71(1)}Er_{0.29(1)}FeO_3$	$CaTiO_3$	$cP5$	Pm-$3m$	52.8
	$Er_{0.91(2)}Sr_{0.09(2)}FeO_3$	$GdFeO_3$	$oP20$	$Pnma$	42.6
	Er_2O_3	$(Mn_{0.5}Fe_{0.5})_2O_3$	$cI80$	Ia-3	4.6
$Sr_{0.5}Tm_{0.5}FeO_3$	$Sr_{0.71(1)}Tm_{0.29(1)}FeO_3$	$CaTiO_3$	$cP5$	Pm-$3m$	57.2
	$TmFeO_3$	$GdFeO_3$	$oP20$	$Pnma$	42.8
$Sr_{0.5}Yb_{0.5}FeO_3$	$Sr_{0.72(1)}Yb_{0.28(1)}FeO_3$	$CaTiO_3$	$cP5$	Pm-$3m$	56.7
	$YbFeO_3$	$GdFeO_3$	$oP20$	$Pnma$	43.3
$Sr_{0.5}Lu_{0.5}FeO_3$	$Sr_{0.74(1)}Lu_{0.26(1)}FeO_3$	$CaTiO_3$	$cP5$	Pm-$3m$	53.8
	$LuFeO_3$	$GdFeO_3$	$oP20$	$Pnma$	46.2

References

[1] P. Wagner, G. Wackers, I. Cardinaletti, J. Manca, J. Vanacken, *Phys. Status Solidi A* **9**, 1700394 (2017).

[2] R.J.D. Tilley, *Perovskites Structure-Property Relationships*, John Wiley & Sons, UK 2016.

[3] S. Thomas, A. Thankappan, *Perovskite Photovoltaics. Basic to Advanced Concepts and Implementation*, Academic Press, Elsevier, 2018.

[4] P. Villars, K. Cenzual, Pearson's Crystal Data, Crystal Structure Database for Inorganic Compounds, ASM International, Materials Park (OH), 2019/2020.

[5] V.V. Hrytsan, O.I. Zaremba, R.E. Gladyshevskii, *Visn. Lviv. Univ. Ser. Khim.* **62**, 99 (2021).

[6] D.B. Wiles, A. Sakthivel, R.A. Young, Program DBWS3.2 for Rietveld analysis of X-ray and neutron powder diffraction patterns, School of Physics, Georgia Institute of Technology, Atlanta (GA) 1998.

[7] C.H. Yo, I.Y. Jung, K.H. Ryu, K.S. Ryu, J.H. Choy, *J. Solid State Chem.* **114**, 265 (1995).